

# Do accretion discs regulate the rotation of young stars?

S. P. Littlefair<sup>1</sup>, Tim Naylor<sup>1</sup>, Ben Burningham<sup>1</sup>, R. D. Jeffries<sup>2</sup>

<sup>1</sup>*School of Physics, University of Exeter, Exeter EX4 4QL, UK*

<sup>2</sup>*School of Chemistry and Physics, Keele University, Keele, Staffordshire, ST5 5BG, UK*

Submitted for publication in the Monthly Notices of the Royal Astronomical Society

18 November 2018

## ABSTRACT

We present a photometric study of *I*-band variability in the young cluster IC 348. The main purpose of the study was to identify periodic stars. In all we find 50 periodic stars, of which 32 were previously unknown. For the first time in IC 348, we discover periods in significant numbers of lower-mass stars ( $M < 0.25M_{\odot}$ ) and classical T-Tauri stars. This increased sensitivity to periodicities is due to the enhanced depth and temporal density of our observations, compared with previous studies. The period distribution is at first glance similar to that seen in the Orion Nebula Cluster, with the higher-mass stars ( $M > 0.25M_{\odot}$ ) showing a bi-modal period distribution concentrated around periods of 2 and 8 days, and the lower-mass stars showing a uni-modal distribution, heavily biased towards fast rotators. Closer inspection of the period distribution shows that the higher mass stars show a significant dearth of fast rotators, compared to the Orion Nebula Cluster, whilst the low mass stars are rotating significantly faster than those in Orion. We find no correlation between rotation period and  $K - L$  colour or  $H\alpha$  equivalent width.

We also present a discussion of our own IC 348 data in the context of previously published period distributions for the Orion Nebula Cluster, the Orion Flanking Fields and NGC 2264. We find that the previously claimed correlation between infrared excess and rotation period in the ONC might in fact result from a correlation between infrared excess and *mass*. We also find a marked difference in period distributions between NGC 2264 and IC 348, which presents a serious challenge to the disc locking paradigm, given the similarity in ages and disc fractions between the two clusters.

**Key words:** accretion, accretion discs, stars:pre-main-sequence planetary systems: protoplanetary discs

## 1 INTRODUCTION

The question of the early evolution of stellar angular momentum is an interesting and essentially unsolved problem. It is well known that a substantial number of young stars show spin rates well below their break-up speed (e.g. Bouvier et al. 1993), despite the fact that these stars should spin up as they contract towards the main sequence. Furthermore, the angular momentum distributions of older stellar clusters such as the Pleiades, and the simultaneous presence of ultrafast rotators and slowly rotating stars amongst solar-type stars, argue for a phase of angular momentum regulation amongst pre-main-sequence stars (Barnes et al. 2001; Tinker et al. 2002). The most promising mechanism to regulate the angular momentum of young stars is disc-locking - a proposal first put forward by Koenigl (1991). In

the disc locking theory, magnetic field lines connect the star to the disc, enforcing synchronous rotation between the star and the material in the disc at some radius, near where the magnetic field disrupts the disc.

However, observational and theoretical support for disc locking is still controversial. Whilst evidence exists that some young stars possess the kilogauss-strength magnetic fields necessary to disrupt the accretion flow (e.g. Johns-Krull et al. 1999), theoretical arguments by Safer (1998) and Matt & Pudritz (2004) have called into question the effectiveness of disc locking. Furthermore, Hartmann (2002) argues that, even if disc locking is effective, it may take almost 1 Myr to affect the angular momentum of a young star. Observationally, evidence for disc locking is ambiguous. In the Orion Nebula Cluster (ONC), the most heavily studied region to date, studies of rotation rates were ini-

tially conflicting. Whilst Attridge & Herbst (1992) and later Choi & Herbst (1996) found a bi-modal period distribution amongst the young stars, Stassun et al. (1999) argued that the distribution was not significantly different from uniform. The source of this conflict has now been resolved - the period distribution in the ONC is mass-dependent. Whilst the brighter stars show a bi-modal distribution, the fainter stars (which dominate the study of Stassun et al. 1999) show a uni-modal distribution.

In addition to a bi-modal period distribution, Herbst et al. (2002) also report a strong correlation between rotation rate and infrared excess, and suggest that the ONC therefore provides a strong argument for the reality of disc locking. This confirms the findings of earlier studies, which found significant differences in rotation rates between stars still surrounded by circumstellar discs and those that lack evidence for discs (e.g. Edwards et al. 1993). However, other studies of rotation rates fail to show statistically significant differences between stars which show and stars which lack disc signatures (e.g. Stassun et al. 1999; Rebull 2001; Rebull et al. 2002; Makidon et al. 2004). Furthermore, we argue in this paper that the correlation between infrared excess and rotation rate, as seen by Herbst et al. (2002), might in fact be a consequence of the dependence of rotation rate upon stellar mass (see section 4.4). A lack of any correlation between disc presence and rotation rate is a serious challenge to disc locking.

Here we present a study of the photometric variability of stars in the young cluster IC 348. IC 348 is nearby and extremely young. Its distance is 260 pc from *Hipparchos* parallaxes or 316 pc if main-sequence fitting is used (Scholz et al. 1999; Herbig 1998). Based upon isochronal fitting of the pre-main sequence, the median age of the cluster is between 1.3 and 3 Myr (depending upon the distance adopted). The membership status of stars towards IC 348 is well established by a major spectroscopic census (Luhman et al. 2003). These factors make IC 348 an ideal cluster in which to study the rotation of young stars. Importantly, IC 348 is older than the well studied ONC region, and therefore should allow a determination of timescales involved in disc locking. Indeed, IC 348 has already been photometrically monitored, with the aim of determining rotation periods (Herbst et al. 2000; Cohen et al. 2004). However, the relatively shallow nature of these studies means that few periodic variables were discovered, hampering the ability of those studies to make statistically significant conclusions. The study presented here re-visits IC 348 with deeper photometry with the aim of increasing the number of known periodic variables in IC 348.

In section 2 we present the observations and data reduction techniques applied. Section 3 characterises the internal accuracy of our dataset, and describes some of the more interesting irregular variables. Section 4 describes the techniques used to identify periodic variables and the results of our study. Finally, in section 5 we compare the period distribution found for IC 348 with other published period distributions, and draw our conclusions.

## 2 OBSERVATIONS AND DATA REDUCTION

### 2.1 Observations

RGO *I*-band CCD images were taken with the CCD imager on the Jacobus Kapteyn Telescope (JKT) on La Palma, equipped with a single 2048×2048 pixel SITe array. The imager covers approximately 14 × 14 arcmin on the sky, however only the central 9 × 9 arcmin is useable for accurate photometry, as the edges of the imager suffer from strong vignetting. A single field, centred on IC 348 ( $\alpha = 3^h 44^m 28.5^s$ ,  $\delta = +32^d 08^m 36^s$  J2000) was observed, with data being taken on every night between 28/29th December 2002 and 9/10th January 2003, with additional imaging on the nights beginning 19th–22nd January 2003. The number of nights on which data were taken totalled seventeen, and covered a baseline of twenty-six days. The seeing varied between 0.8 and 3", with a median and standard deviation of 1.3" and 0.4" respectively. Most nights were affected by thin to heavy cirrus cloud, although the nights beginning on 12th December 2002, 3rd January 2003 and 6th January 2003 were photometric. To increase the dynamic range of the resulting study, we used exposure times of 2, 30 and 3×300 seconds which were repeated many times throughout a night. This yielded between 10 and 20 observations with the short and medium exposure times and between 30 and 60 observations with the long exposure time per night. In total we obtained 227 useable short exposures, 230 useable medium exposures and 607 useable long exposures.

### 2.2 Image Processing and Optimal Photometry

The individual frames were bias subtracted using a median stack of several bias frames. In most cases bias frames taken on the same night were used, with the exception of the 31st December and the 1st January, where the bias frames were affected by stray light from the dome. The frames were then flat fielded using twilight sky flats taken on one of the photometric nights. Only sky flats with peak counts of less than 30,000 were used, to avoid non-linearity effects. The CCD was affected by a number of bad columns and pixels. A bad pixel mask was constructed for all frames by flagging all pixels which deviated by more than  $10\sigma$  from the median of a ratio of two flat fields. In addition, a smoothed version of a long exposure was subtracted from the long exposure, and all pixels with a value lower than 1000 were masked. These procedures accounted for most bad pixels, but left a number of bad columns unmasked. These columns were identified by hand and added to the bad pixel mask.

The processed CCD frames were then analysed using optimal photometry, as implemented by a slightly modified version of the CLUSTER software described in detail by Naylor et al. (2002). Advantages of this approach over classical aperture photometry include better signal-to-noise ratios, and robustly determined uncertainties for each observation. Firstly, we summed the exposures from the night of 6th January 2003 (the night which had the best seeing), after correcting for positional shifts to form a deep *I*-band image which was then searched for objects. Only stars with a signal-to-noise ratio threshold of 15 in the summed image were retained, low enough to detect all the stars for which good photometry would be obtained in the 300 second exposures, but high enough to prevent spurious detections.

We note here that, as we are only interested in the high signal-to-noise ratio data required to detect the small periodic variations in T-Tauri stars, all stars with a mean signal-to-noise in a single 300s image of less than 50 were removed from the final catalogue. This corresponds to a magnitude cut at  $I=18$ . The shifts between each individual frame, and the summed  $I$ -band image were then parameterised with a 6-coefficient solution, and optimal photometry (see Naylor 1998) was performed for every object in each frame. Because the signal-to-noise of our images was high, we fitted the positions of each object independently for each frame.

In classical aperture photometry, an aperture correction is used to correct the flux measured in the small apertures used for the objects, to the large apertures used for standard stars. There is an analogous process in optimal photometry, known as “profile correction”. Bright, unsaturated stars in each frame were used to derive the profile correction which was applied to the optimal photometry values. Surprisingly, given the small field of view of the JKT imager, we found that this profile correction must be allowed to vary as a quadratic function of position, implying that the PSF of the CCD imager on the JKT is spatially variable. The spatially varying PSF of the CCD imager would affect relative aperture photometry too, as the aperture correction would also need to vary with position.

An important aside arises regarding *relative* photometry. It is often assumed that there is no need to account for this effect in relative photometry, because the position of a star is usually constant on the CCD. Although the aperture or profile correction may indeed vary with position, the error so introduced therefore should remain constant for any given object, and so the relative photometry will still be correct. We find that this assumption is wrong because, crucially, the seeing will vary between observations. At times where the seeing is poor, the variable PSF of the instrument will be swamped by bad seeing, and the aperture correction will be constant across the frame. At times where the seeing is good however, the variable PSF of the instrument becomes important again. If the aperture or profile corrections are not allowed to vary as a function of position and time, therefore, such behaviour will lead to implied variability, even for constant objects. It is therefore crucial to allow the aperture or profile correction to be spatially variable, even for relative photometry on small-field imagers like the JKT. Failure to account for this affect likely explains the “variable” stars found around the edge of the field in the recent study of Lamm et al. (2004).

After profile correction, the photometric measurements were adjusted for any difference in the airmass and transparency for each frame, by determining a relative transparency correction from the bright stars. A critical step in the determination of the transparency correction is the identification of stars whose average magnitude will define the reference brightness for each frame. Our reduction differs from that described in Naylor et al. (2002), in that this process was performed iteratively. First, we used all stars with good measurements and signal-to-noise ratios larger than 10 to define a reference magnitude. Then we reject all stars with large scatter, signal-to-noise ratios lower than 10 or a small number of good measurements and recompute a reference magnitude. This process was repeated until the  $\chi^2_\nu$  of the remaining stars was less than 2. Before this process we

added an additional, magnitude-independent error of 0.01 to the results of each frame, in order to yield a plot of  $\chi^2_\nu$  versus signal-to-noise ratio that was flat and had a modal value of approximately 1. The transparency correction was applied to all observations, with airmasses ranging from 1 to 3. In the absence of colour information, errors may be introduced into our relative photometry by the colour dependence of extinction. The following simulation was performed to estimate the importance of this effect. By cross-correlation with the photometry of Herbig (1998) we find that the stars used to determine the transparency correction have  $R-I$  colours between 1.5 and 3, whereas the stars in our catalogue have  $R-I$  colours between 1 and 3. We compared the  $I$ -band magnitudes of two stars with  $R-I$  values of 1.5 and 3.0. Simulating their spectra as linear fits between the fluxes at the mid-points of the two bands and folding them through the responses of the Earth’s atmosphere, the telescope, filter and CCD, we found that their relative  $I$ -band magnitudes changed by 3mmags between an airmass of 1 and 3. Hence we are confident this effect is negligible for the purpose of our analysis.

An astrometric solution was achieved through comparison with a 2MASS catalogue of the same region. A 6-coefficient solution to 144 stars yielded a rms discrepancy in positions of 0.06 arcseconds. No astrometric distortion model was included, and the position discrepancies showed no systematic trends, implying that the JKT imaging system is astrophotographic to an accuracy of at least 0.06 arcseconds.

There are three further departures from the methods outlined in Naylor et al. (2002), worthy of note.

(i) We have altered the way in which the  $I$ -band magnitude is “flagged” in order to describe the quality of a single data point. We now use character based flags according to the scheme laid out in Burningham et al. (2003). In addition, we have added a flag to denote observations which fall within the heavily vignetted region of the CCD, which we label with the character R.

(ii) To reduce the effect of cosmic ray hits upon the lightcurves presented here, we remove such events by making an additional test for non-stellarity (following the methods outlined in Naylor et al. 2002) upon every star in each frame. A star which is affected by cosmic ray hits will fail this non-stellarity test, and the measurement for this image is flagged with the character N.

(iii) The sky estimation technique is robust to the presence of nearby stars inside the sky box or smooth gradients in the sky background. However, curvature in the sky background, as might be introduced near bright stars or in the vignetted regions of the CCD, will result in a histogram of pixel values that is highly asymmetric and not well fit by the skewed Gaussian model we adopt. We therefore demand that the  $\chi^2_\nu$  of the fit to the sky histogram is less than 4, and that the skewness parameter is less than 0.3. If either of these conditions is not satisfied an ill-determined sky flag (I) is set.

### 2.3 Transformation to a standard system

Our aim in obtaining this dataset was to obtain high standard relative photometry of IC 348. This meant that we did not obtain colour information for each star at each epoch,

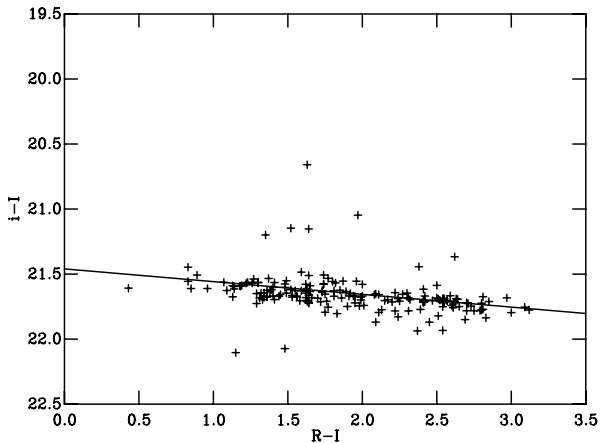


**Figure 1.** Difference between our instrumental magnitude  $i$  and standard magnitude on the Cousins system measured by Herbig (1998) as a function of colour. A linear least-squares fit to the data is shown.

and hence we are unable to tie our photometry to a standard system directly. Instead, we tied our photometry to the photometric system of Herbig (1998). The Herbig (1998) catalogue contains photometry of all the stars towards IC 348, which was in turn tied to the Cousins system by observations of standard stars from the list of Landolt (1992). The difference in our instrumental magnitude  $i$ , against standard magnitude  $I$ , from Herbig (1998) is shown in figure 1. The linear, least-squares fit gives the following relationship between Cousins  $I$ -band magnitude and instrumental  $i$ :

$$I = i + 21.46 + 0.098 \times (R - I). \quad (1)$$

In the absence of colour information, we simply used an average  $R - I$  value of 2.0 to convert our instrumental magnitudes to Cousins  $I$ . Whilst not ideal, figure 1 shows that it provides  $I$ -band magnitudes correct to around 0.3 mags. This should be borne in mind when comparing this catalogue to others in the literature.

## 2.4 Final Dataset

The final data set consists of lightcurves for 169 stars, with  $I$ -band magnitudes brighter than  $I=18$ . Rather than combine data with very different sizes of error bars, three lightcurves were produced for each star, resulting from the 300, 30 and 2 second exposures. From the 300 second exposures, 138 stars have lightcurves with a median signal-to-noise ratio of 10 or more, and at least 30 unflagged datapoints. For the 30 second exposures, a further 15 stars satisfy the same criteria. The 2 second exposure satisfy the same criteria for an additional 9 stars.

The best quality lightcurve for each star, along with positions, mean  $I$ -band magnitudes, and periodograms are available electronically via Centre de Données astronomiques de Strasbourg (CDS), and also from the Cluster collaboration homepage (<http://www.astro.ex.ac.uk/people/timm/Catalogues/description.html>).

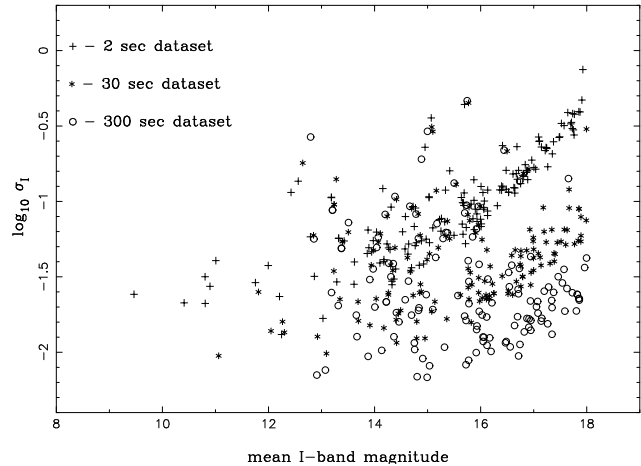


**Figure 2.** Scatter in the photometry of stars as a function of brightness. Different symbols correspond to data from different exposure times.

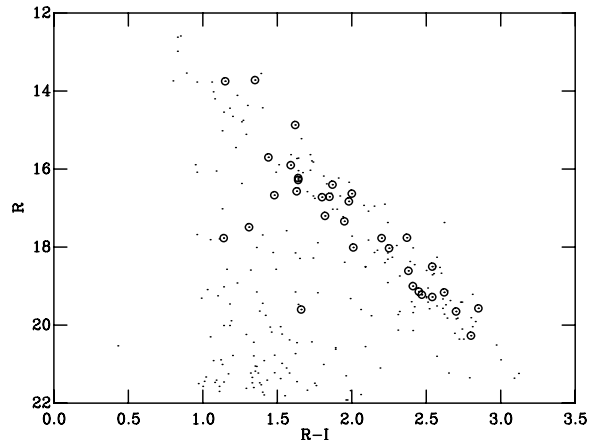


**Figure 3.** Colour magnitude diagram of IC 348. Circles represent variable stars.

## 3 VARIABILITY

Figure 2 shows the RMS variability in magnitudes for our stars, plotted as a function of magnitude. This plot shows the high internal accuracy reached in our dataset. The 30 second and 300 second exposures have an internal accuracy of around 0.01 mags. The 2 second dataset is somewhat poorer, with an internal accuracy of only 0.02 mags. The most likely explanation for this is that the 2 second dataset had relatively few stars suitable for use in determining the transparency correction for each frame. Typically, around 17 stars were available for this, but the number of suitable stars was sometimes as low as five or six.

We could use the RMS variability as a means of detecting variable stars, however the availability of robust error determinations for our measurements makes  $\chi^2_\nu$  a more useful measure of variability. We have described a star as variable if  $\chi^2_\nu > 2.5$  (the probability that this value of  $\chi^2_\nu$  might arise by chance in a non-variable star obviously depends upon the number of good data points, but is always less than 1%).

As an aside, we note that variability is an excellent way of discovering pre-main sequence stars. Figure 3 shows the  $R$ -band magnitude and  $R-I$  colours (as determined by Herbig 1998) of the variable stars in our survey. The vast majority of the variable stars lie in the pre-main sequence region.

### 3.1 Irregular Variables

Forty-three stars are irregular variable stars (showing  $\chi^2_\nu > 2.5$  and with no detected period). The standard picture of variability in T-Tauri stars (see Herbst et al. 1994, for example), predicts that classical T-Tauri stars are more highly variable and erratic than the weak-lined T-Tauri stars, because of the presence of variability from accretion. As the magnitude distribution of CTTs and WTTs are similar in our dataset, we can perform a direct comparison of variability between the two groups to test this prediction. We note here that we have classified the stars as weak-lined or classical based upon the  $H\alpha$  equivalent width measurements presented in Luhman et al. (2003). Stars with  $H\alpha$  equivalent widths greater than  $10\text{\AA}$  are classified as classical T-Tauri stars, otherwise a star is classed as weak-lined.

Overall, the variability seems to support the standard picture of variability in T-Tauri stars. The classical T-Tauri stars are more highly variable than the weak-lined T-Tauri stars, with the CTTs showing an average standard deviation of 0.1 mags, compared with 0.05 mags for the WTTs. However, the CTTs are just as likely to be non-variable as the WTTs - the ratio of CTTs to WTTs amongst the non-variable stars is  $0.41 \pm 0.1$ , which is not different from the ratio of CTTs to WTTs in the cluster as a whole. Figure 4 shows lightcurves for the most highly variable classical T-Tauri stars. The variability reaches amplitudes as high as 1.5 mags (star 40), and is characterised by erratic flickering. The most likely source of this variability is irregular accretion onto the young star.

Somewhat surprisingly then, large amplitude variability is not restricted to the classical T-Tauri stars. Out of the 43 irregular variables found, 23 are weak T-Tauri stars, and six weak-lined T-Tauri stars show large amplitude variability ( $\chi^2_\nu > 20.0$ ). These stars are shown in figure 5. The amplitudes and characteristics of the variability in these stars are similar to those seen in the CTTs. Two stars are unusual and worthy of further mention. Star 67 (Herbst 47) was seen by Cohen et al. (2004) to change from being periodic with a period of 8.4 days to showing large erratic dips of up to 1 mag. These dips are interspersed with long intervals near maximum brightness. Our lightcurve shows the same erratic behaviour. This behaviour is characteristic of UX Ori stars (see Herbst et al. 1994). UX Ori type behaviour is usually attributed to occultations of the central star by disc material, and it is therefore highly unusual for such behaviour to be seen in a weak-lined T-Tauri star. Star 96 (Herbst 73) was included as a periodic star in Cohen et al. (2004), with a period of 7.6 days. The star is not included in our periodic sample, because the  $\chi^2_\nu$  with respect to a sinusoidal fit is too large. However, given that we find a period of 7.2 days for this star, it clearly is periodic, and furthermore the period is stable over several years. It is difficult to explain the behaviour of star 96 in terms of starspots and stellar rotation, however. The star remains at maximum brightness for over four days, then suddenly drops in flux by over 50%, recov-

ering its flux around 3 days later. We believe the behaviour of this star may be due to eclipses by extended, long-lived structure in an accretion disc around the star. Similar behaviour (albeit with a much longer period) has been explained in this manner for the star KH 15D (Hamilton et al. 2001).

It is tempting to link the variability of stars 96 and 67 to the presence of a circumstellar disc. The presence of a circumstellar disc in these objects is confirmed by the presence of a  $K-L$  excess (Haisch et al. 2001). However, these are weak-lined T-Tauri stars, which are traditionally thought to lack discs. In fact, a strong body of evidence is emerging that a significant fraction of stars classified as weak-lined T-Tauri stars do possess discs: the eclipses in KH 15D are strongly indicative of eclipses by disc material (Hamilton et al. 2001) and infrared excesses have been seen around a large number of weak-line T-Tauri stars (Gregorio-Hetem & Hetem 2002). In addition, Littlefair et al. (2004) claim that the composite spectrum effect, first seen by Bouvier & Appenzeller (1992) in a group of four weak-lined T-Tauri stars, is caused by high accretion rates, which necessarily implies the presence of an accretion disc.

## 4 PERIODIC VARIABLES

### 4.1 Detection of Periodic Variables

In identifying periodic variables, our aim was to detect the largest number of periodic variables possible, whilst keeping the fraction of spurious detections suitably low. Traditional methods of estimating the significance of a detected signal (Horne & Baliunas 1986; Linnell Nemeč & Nemeč 1985) are not applicable to our dataset. The method of Horne & Baliunas (1986) is strictly applicable only to evenly spaced, uncorrelated datapoints (see Herbst & Wittenmyer 1996), whilst the method of Linnell Nemeč & Nemeč (1985) is not valid for correlated datapoints. Night-to-night variations in our data (e.g. transparency corrections, non-periodic stellar variability) will make our datapoints strongly correlated; our datapoints are, by necessity, unevenly spaced.

As there is no formally correct way to calculate the significance of our detected periods, we use a modified version of the procedure detailed in Herbst et al. (2000). Two periodograms are calculated for each star, using the method formulated by Horne & Baliunas (1986). One periodogram is based upon the whole lightcurve, the other based upon a modified dataset consisting of the weighted mean of each night's data. This latter dataset is much closer to the ideal of evenly spaced, uncorrelated data, and it is reasonable to use it with the method of Horne & Baliunas (1986) to calculate a false alarm probability (FAP) for the period found in the original dataset. In principle it is now possible to differentiate between real and spurious periods by making a cut at some value of the FAP. What value of the FAP to use is necessarily a subjective decision. Naylor and Littlefair independently classified the period detections based upon visual inspection of the folded lightcurves from the 300s dataset. The period detections were grouped into three categories; certain, uncertain and spurious. The distribution of the FAP for each category was examined. In both cases, few "certain" detections had FAPs greater than 0.08. However, there were

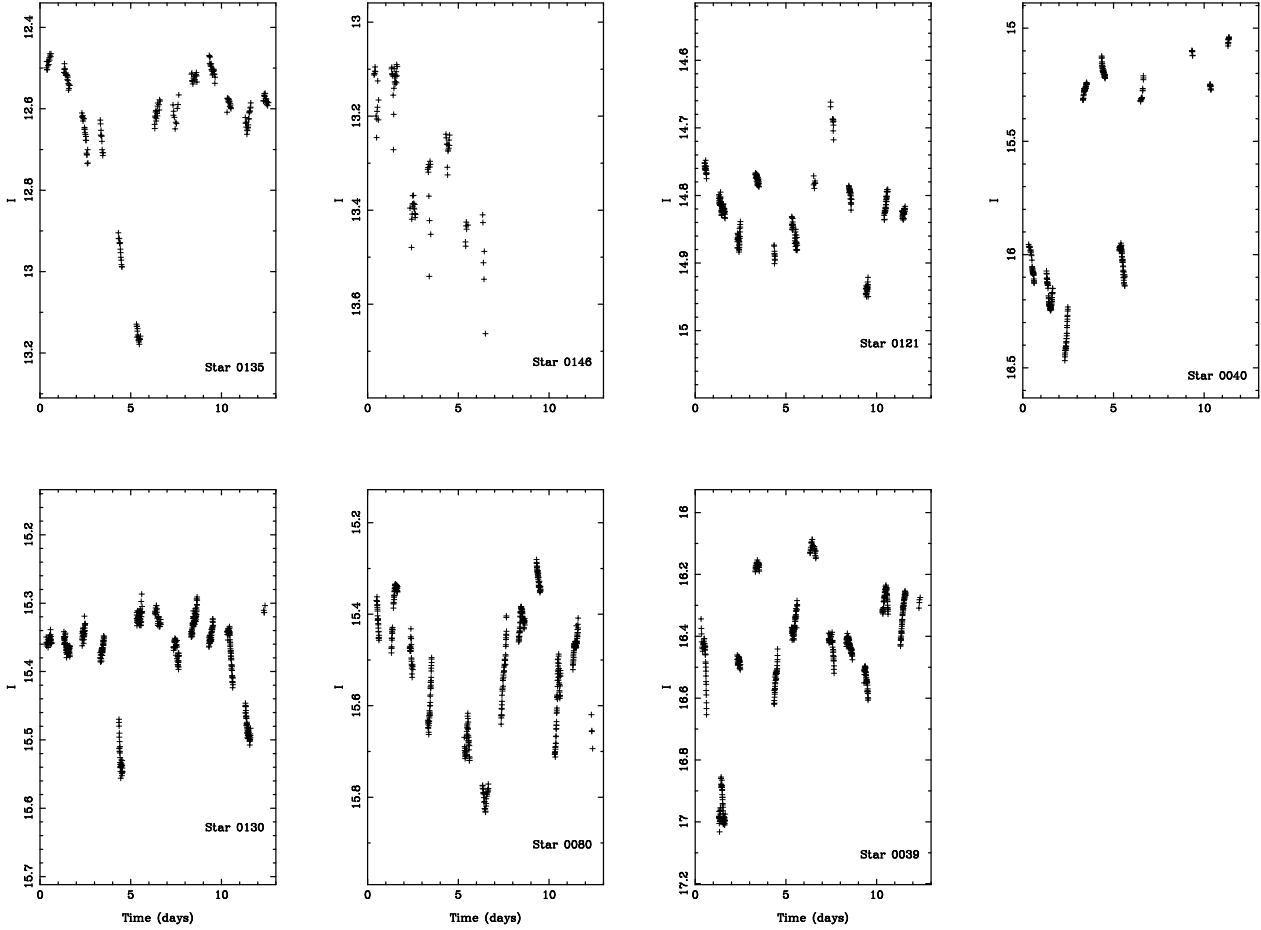


**Figure 4.** Lightcurves of the most variable non-periodic CTTs. All classical T-Tauri stars with  $\chi^2_\nu > 20.0$  are shown.

a substantial number of “spurious” and “uncertain” detections below this point.

We were reluctant to use a lower FAP as our cut-off, as this meant throwing away many detections independently classified as “certain”. Instead, we looked at the lightcurves of the “spurious” and “uncertain” stars which had passed our FAP cut-off to see if there were some other criteria we could use to reject these stars. The majority of “spurious” and “uncertain” detections were lightcurves in which the amplitude of any variability was small or negligible. A small number of “spurious” and “uncertain” detections were highly erratic, large amplitude variables, and a further number were stars whose detected periods were too long to be classed as “certain”. Additionally, some stars had too few data points, or the folded lightcurves covered only a small fraction of the rotational cycle. To filter out these objects we computed a third periodogram for all stars, using a sinusoid fitting technique. At each period to be considered, a sine-curve is fit to the data, and the resulting value of  $\chi^2_\nu$  is calculated. The detected period is taken to be the period which minimises the value of  $\chi^2_\nu$ . After calculating this periodogram, we rejected those stars with  $\chi^2_\nu > 15^1$ , stars with

periods longer than 14 days, stars whose lightcurves had less than 50 data points, or whose folded lightcurve had gaps of more than 0.25 of a rotational cycle. We also characterised the amplitude of variability by the amplitude of the sine-fit  $a$ . Stars with  $a \geq 18\sigma_m/\sqrt{N_p}$ , where  $N_p$  is the number of data points, and  $\sigma_m$  the median uncertainty in flux, were rejected. Also rejected were stars with periods between 0.9 and 1.1 days.

The above procedure, derived from the 300s lightcurves alone, was applied, without modification, to all three datasets. The 300 second lightcurves yielded 42 periodic variables. The 30 second lightcurves yielded 37 periodic variables, of which 8 were not found in the 300 second dataset. These 8 stars had lightcurves with a large number of saturated points in the 300 second dataset. The 2 second lightcurves yielded 18 periods, all of which were present in either the 300 second or 30 second dataset. As a check that our period detection process was not yielding significant numbers of spurious detections, we examined the periods of those stars which shared detections across datasets. In all cases, the periods agreed to within 10% of each other. For the purposes of this paper, the period adopted was the value computed from the longer exposure dataset, via the

<sup>1</sup> To ensure that the  $\chi^2_\nu$  cut-off was not rejecting stars which were clearly periodic but non-sinusoidal, all the stars rejected because of  $\chi^2_\nu$  criteria were inspected by hand. Only one periodic object,

star 96, was rejected on the basis of  $\chi^2_\nu$ . This star is discussed in detail in section 3.1

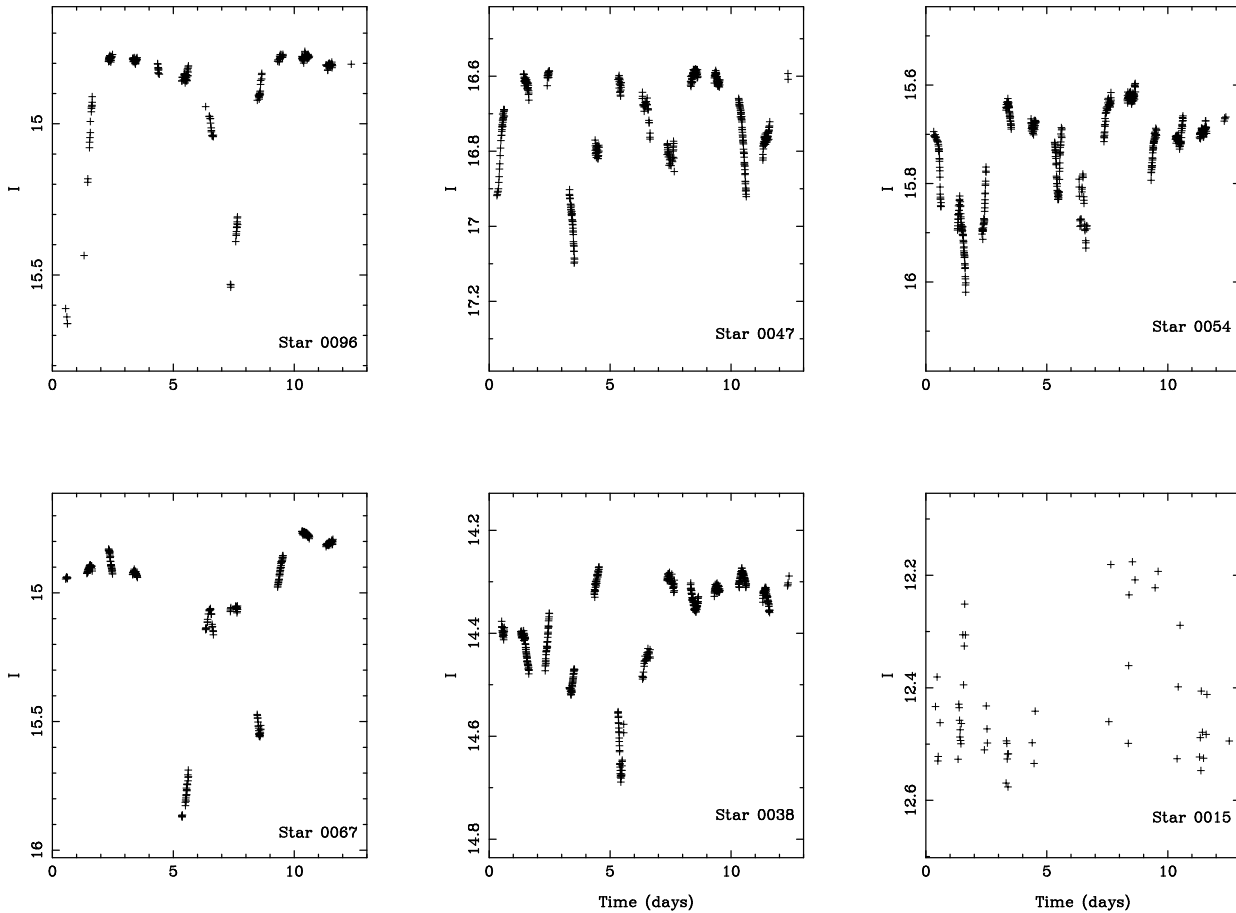


**Figure 5.** Lightcurves of the most variable non-periodic WTTs. All weak-lined T-Tauri stars with  $\chi^2_{\nu} > 20.0$  are shown.

sine-fitting method. In total, 50 periodic variables were identified. These stars are shown in table 1. Periodograms from the sine-fitting method are available online, as are the folded lightcurves.

#### 4.2 Comparison with previous work

Prior to this work, data on rotation periods in IC 348 have been published in Cohen et al. (2004). This study is based on observations spread over five observing seasons with the 0.6m telescope at the Van Vleck Observatory, and yields total of 28 known periodic stars (a subset of this dataset was published in Herbst et al. (2000)). Of the 50 periodic stars presented here, 18 were previously known, and the remaining 32 are new. Our study therefore more than doubles the number of known periodic variables in IC 348. Ten periodic stars from Cohen et al. (2004) were not recovered in this study, seven of which are within our field of view. Five of these seven stars were not identified as periodic because they fail our false alarm probability criterion. Of these five stars, four stars show periods which either agree with Cohen et al. (2004), or are explained by aliasing or doubling (see figure 6). This fact suggests that our selection criteria for periodic stars is more conservative than that employed by

Cohen et al. (2004)<sup>2</sup> The remaining two stars (stars 96 and 67) were rejected because they failed our  $\chi^2_{\nu}$  criterion. These stars are discussed in detail in section 3.

The periods found for the 18 stars in common between this study and the study of Cohen et al. (2004) are shown in figure 6. The large majority of period determinations agree. This suggests that rotation periods in young stars are stable over periods of five years or so, confirming the results seen by Cohen et al. (2004). Figure 6 also allows us to estimate the uncertainties on our period determinations. Below periods of 10 days, the period determinations agree to better than 0.1 days. We conclude that our periods are at least this accurate. The plot shows increasing scatter with increasing period. This is due to the comparatively short monitoring time in this study, leading to a lower accuracy in periods longer than 10 days. One period is consistent with a beat period between the real period and the sampling interval of  $\sim 1$  day, and a single star shows a disagreement in the claimed periods. This star (star no. 74 in this paper; Herbst's star no. 12) exhibits a period of 2.2 days in Cohen et al. (2004), and 10.8 days in this study. Whilst we are unable

<sup>2</sup> This conclusion is not affected by the fact that we have discovered many additional periods to those found by Cohen et al. (2004). The new periods presented here are predominantly in low mass stars, for which the photometry of Cohen et al. (2004) would not have been sufficiently deep to detect periods.

**Table 1.** Periodic variables in IC 348.  $\chi^2_{\nu}$  is determined with respect to the best fitting sinusoid. H $\alpha$  equivalent width measurements are taken from Luhman et al. (2003). A value of 0.0 indicates that no H $\alpha$  emission was detected or measurable. The masses are determined using the method described in section 4.2.

Star ID	Cohen ID	Period (days)	$I$	$\chi^2_{\nu}$	SpT	EW H $\alpha$ (Å)	Mass ( $M_{\odot}$ )
4	50	5.36	13.338	0.52	K5	1.5	
5	88	13.69	15.747	5.47	M2	22.0	0.33
7	69	3.27	15.329	4.73	M4.5	6.5	0.17
10	37	14.00	14.332	6.31	M4	5.5	0.18
11	34	8.43	14.615	4.97	M1	90.0	0.43
20	86	1.39	15.902	8.26	M5.25	3.0	0.16
21	133	6.31	15.076	1.51	M0	51.0	0.53
25		1.33	17.324	0.97	M4.75	3.0	0.19
31	39	10.16	14.199	0.69	M2.5	4.0	0.28
35		1.73	17.827	1.08	M5.75	140.0	0.13
36		1.50	17.712	1.11	M5.25	7.0	0.16
41	82	3.74	14.732	0.45	M4.75	4.0	0.17
45	16	5.21	13.189	1.58	K6	3.9	0.44
48	60	6.96	14.643	1.97	M1.5	0.0	0.38
50	96	1.52	16.095	0.45	M5	5.0	0.17
52	98	3.58	16.935	6.03	M4.25	50.0	0.18
55	26	3.01	12.801	1.15	K0	0.0	1.34
56	81	3.98	14.768	1.15	M2	8.0	0.32
58	105	1.73	15.703	0.75	M5	7.0	0.17
60	14	1.63	12.203	0.70	G8	0.0	
65		0.57	17.550	2.18	M7.5	15.0	0.06
69	46	2.09	14.389	0.54	M3.25	3.0	0.23
70	43	6.68	14.344	0.51	M3	5.0	0.24
71		1.77	17.245	0.72	M5.75	6.0	0.15
72	61	2.18	14.815	1.46	M2	47.0	0.33
73	45	2.39	13.883	0.40	K3	0.0	1.01
74	12	10.81	12.241	0.76	K2	0.0	1.27
77	27	2.65	11.755	0.86	G6	0.0	
78	108	2.52	15.689	11.45	M4.75	30.0	0.16
82	29	7.93	14.049	12.14	K7	68.0	0.40
83	142	1.68	16.176	0.55	M5.25	0.0	0.16
84	70	13.04	15.076	1.82	M1.25	10.5	0.15
85	30	7.55	14.184	1.09	M4.75	0.0	0.31
97	74	2.25	16.032	0.46	K6.5	4.5	0.17
98	41	7.12	13.460	0.52	M4.75	1.4	0.57
100	122	1.54	16.676	0.85	M3.5	4.5	0.19
106	134	8.56	15.836	1.47	K5	9.0	0.21
111	51	12.43	13.970	0.60	M1	1.5	0.51
115	135	7.48	15.933	8.23	M2.25	3.0	0.27
117	52	11.22	14.244	1.00	M0	2.0	0.52
126		1.58	16.890	0.71	M5	7.0	0.18
127	64	6.84	15.134	0.93	M2.5	8.0	0.28
131	21	9.11	13.624	0.71	M1	3.5	0.38
141	31	3.08	14.021	1.23	M4.75	10.0	
143	127	2.19	15.756	3.84	M5.75	110.0	0.14
144	32	4.90	15.275	1.39	M1	5.0	0.39
147		1.55	17.644	3.86	M5.5	200.0	0.16
178	107	1.90	16.028	0.57	M5.25	74.0	0.15
179		1.79	17.265	1.02	M4.75	5.0	0.19
188	137	3.40	16.927	0.60	M7.25	45.0	0.09

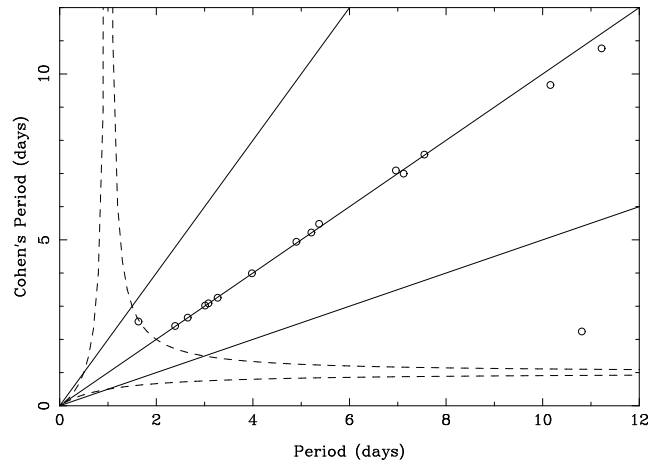


**Figure 6.** A comparison between period determinations in this study and the study of Cohen et al. (2004). The straight lines represent a 1:1 agreement, and factors of two disagreement between the period determinations. A factor of two disagreement may arise if the harmonic of a period is detected instead of the actual period. The dashed lines show periodicities which might be expected due to beating between a real period and the 1 day sampling interval.

to explain the difference in periods for this single star, the agreement in periods between the majority of stars gives us confidence in our period determination procedures.

We were able to allocate masses using the spectroscopy of Luhman et al. (2003) and the isochrones of D’Antona & Mazzitelli (1997) for all 32 of the newly-found periodic objects. The vast majority of these objects are low mass stars. In fact, 87% are lower than  $0.25 M_{\odot}$ . This contrasts strongly with the study of Cohen et al. (2004), where only a single object is below  $0.25 M_{\odot}$ . The increased depth of our study is a simple result of the larger aperture telescope used (1-m versus 0.6-m), and the site quality of La Palma. Also remarkable is the fraction of classical T-Tauri stars discovered to be periodic in our survey. Cohen et al. (2004) notes that in their photometric study, none of the periodic stars found are classical T-Tauri stars, and suggest that this might strongly bias the results of the survey. In contrast, we have found periods in 15 classical T-Tauri stars. In fact the ratio of classical to weak-lined T-Tauri stars amongst our periodic sample is  $0.43 \pm 0.13$ , which is not significantly different from the ratio of classic to weak stars in IC 348 as a whole. It is apparent that our photometric study has been markedly more successful in detecting periods in classical T-Tauri stars than the study of Cohen et al. (2004). Over half of the classical T-Tauri stars in which we find periods are sufficiently bright that Cohen et al. (2004) should also have found periods for these stars. The most likely explanation for this difference is that our study has a very high temporal density of observations, with typical observation spacings of less than ten minutes, and continuous coverage for several nights. The study of Cohen et al. (2004) has much lower temporal density, and several nights can elapse between observations. Because Classical T-Tauri stars are erratically variable on timescales of a few nights, this variability masks the periodic signal in the study of Cohen et al. (2004). The dense spacing of our observations means that this effect is less marked for our survey. We conclude that photometric



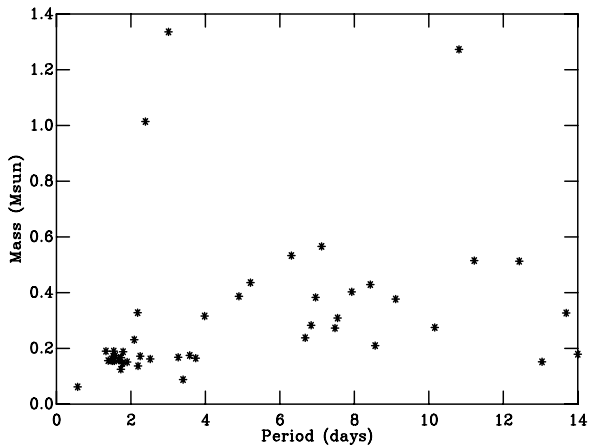


Figure 7. Stellar mass against rotation period.

studies for rotation rates in young stars must have a high temporal density if they are not to be biased by a lack of Classical T Tauri stars.

#### 4.3 Period distribution

Figure 10 shows the period distribution of stars in our sample, where we have split the stars into two groups; those with masses above  $0.25 M_{\odot}$  and those below this mass. For stars with masses greater than  $0.25 M_{\odot}$ , the period distribution in IC 348 appears bi-modal, with peaks around 8 days and 2 days although applying the Hartigan dip test (Hartigan & Hartigan 1995; Hartigan 1995) to the distribution shows that the bi-modality is not statistically significant. The period distribution for the high mass stars resembles the period distribution seen for high-mass stars in the ONC. A K-S test on the periods of the high mass stars in IC 348 and the ONC gives only a 55% probability that the samples were not drawn from the same parent distribution. Both clusters also show broadly similar behaviour for stars with masses below  $0.25 M_{\odot}$  (although differences exist, see below for details). For these stars, the period distribution is clearly unimodal, and the average rotation rate is much higher, with most stars having periods around 1–2 days. A strong correlation between stellar mass and rotation rate is also evident in our study of IC 348 (figure 7). A Spearman Rank Correlation test between stellar mass and rotation period rejects a hypothesis of independence with a confidence of 99.996%. This result shows that the strong mass dependence of rotation rate seen in the ONC (Herbst et al. (2002)) may well be a common feature of young stellar populations. Despite the broadly similar behaviour of rotation period with stellar mass, there is evidence that the rotation period distributions of the low-mass stars in IC 348 and the ONC are different. The low-mass stars in the ONC have a tail of slower rotators extending to periods of over 10 days, whereas the low-mass stars in IC 348 are much more strongly grouped at around 1–2 days. A K-S test of the low mass period distributions in IC 348 and the ONC finds a 98% probability that they are drawn from different parent distributions. In section 5 we present a full discussion of these results, and also com-

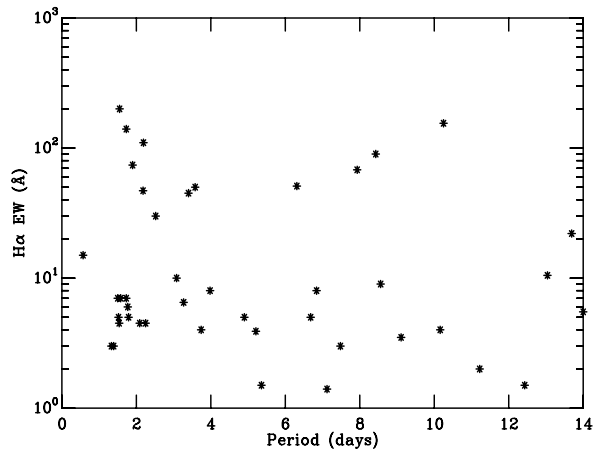


Figure 8.  $H\alpha$  equivalent width against rotation period. Only those 43 stars with a non-zero  $H\alpha$  equivalent width in Luhman et al. (2003) are shown here.

pare the rotation period distribution in IC 348 with those in NGC 2264 and the Orion flanking fields, as well as the ONC.

#### 4.4 Rotation Period and Disc Indicators

The extensive study of rotation rates in the ONC performed by Herbst et al. (2002) showed a strong correlation between rotation period and infrared excess, as judged by  $I - K$  excess. Such a strong correlation would be strongly suggestive that the rotation period distribution in the ONC can be explained by disc locking. However, it may well be that this is merely a secondary correlation, which arises because of the strong dependence of  $I - K$  excess with *stellar mass*. The level of  $I - K$  excess depends upon a number of factors; disc mass, inclination angle, inner disc hole size, and disc structure. It also depends strongly upon stellar mass, with excesses around high mass stars being much stronger than excesses around low mass stars (Hillenbrand et al. 1998). What this means for the ONC is that the low mass stars, which are rotating rapidly, will necessarily exhibit smaller  $I - K$  excesses than the high mass stars, which rotate more slowly. Such an effect could easily be responsible for the apparent correlation between rotation rate and infrared excess. The claims that the ONC offers strong support for disc locking should therefore be interpreted with caution.

As we find a similar period distribution in IC 348 to that seen in the ONC, it is pertinent to ask if we also see a correlation between rotation period and signs of disc presence or accretion. A plot of rotation period against  $H\alpha$  equivalent width is shown in figure 8. Strong  $H\alpha$  emission is a commonly used sign of ongoing accretion onto the central star. We might therefore expect a correlation between  $H\alpha$  equivalent width, and the rotation period of the star, in the sense that actively accreting stars are more likely to be locked to their discs and hence be slow rotators. No such correlation is seen. In fact, a Spearman Rank Correlation test on the two variables rejects the null hypothesis of independence with a probability of only 30%. This result is confirmed

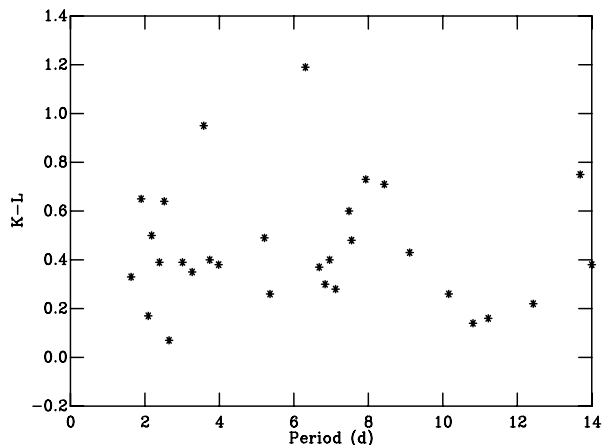


**Figure 9.**  $K - L$  colour against rotation period.  $K - L$  colours are taken from Haisch et al. (2001).

by a K-S test of the period distributions of the classic and weak T-Tauri stars, which gives only a 3% chance the two were drawn from different parent distributions. A similar result arises if we consider the dependence of rotation period against infrared excess, as measured by Haisch et al. (2001) using a  $JHKL$  colour-colour diagram. A star is defined as a  $K - L$  excess source if its  $K - L$  colour places it to the right of the reddening locus of a star at the end of the stellar main sequence (see Haisch et al. 2001, for example). A K-S test of the period distributions of  $K - L$  excess sources and sources with no excess gives a 7% chance that they are drawn from different parent distributions. Likewise, a Spearman Rank Correlation of rotation period against  $K - L$  colour gives a 27% chance that the variables are dependent (see figure 9). We therefore do not find a strong correlation between indicators of inner disc presence and rotation period, nor do we find a strong correlation between rotation period and accretion, as measured by  $H\alpha$  equivalent width.

Smaller sample size is not sufficient to explain the absence of any correlation. To see if a correlation of the strength found in the ONC by Herbst et al. (2002) should be detectable in our sample we randomly selected 50 stars from their dataset, and computed the Spearman Rank Coefficient of  $\Delta(I - K)$  against rotation period. This was repeated many times, and in only 1% of tests was the absolute value of the Spearman Rank Coefficient smaller than that measured between  $K - L$  colour and rotation period for IC 348. We conclude that our sample size is large enough to detect a correlation between  $K - L$  colour and rotation period, provided that correlation was at least as strong as that seen by Herbst et al. (2002) between  $\Delta(I - K)$  and rotation period. In fact, we might expect that the correlation should be even stronger when using  $K - L$  as a diagnostic of disc presence, as we might expect  $K - L$  to be more sensitive to the presence of discs. The most likely explanation as to why we see no correlation is that the  $K - L$  colour is not mass dependent in the same way as  $\Delta(I - K)$ . This is because lower mass stars will exhibit smaller  $K - L$  excesses, but also larger intrinsic  $K - L$  colour, and these two effects will cancel each other out to some extent.

## 5 DISCUSSION

### 5.1 Stars with masses greater than $0.25 M_{\odot}$

The rotation period distributions for IC 348 (this sample), the ONC, the Orion flanking fields (OFF) and NGC 2264 are shown in figure 10. We first discuss the period distributions of the higher mass ( $M > 0.25 M_{\odot}$ ) stars. Above  $0.25 M_{\odot}$ , the ONC period distribution is bi-modal, with peaks at 2 days and 8 days. This bi-modality is highly significant. The Hartigan dip test (Hartigan & Hartigan 1995; Hartigan 1995), gives only a 0.4% chance that the ONC distribution is consistent with a unimodal distribution. This bi-modal distribution, and the correlation between infrared excess and rotation rate, led Herbst et al. (2002) to conclude that disc locking explained the period distribution in the ONC. By modelling the period distribution in the ONC, and assuming that disc locking held stars at periods near to eight days, Herbst et al. (2002) showed that the period distribution in the ONC was consistent with 20–50% of stars in the ONC being locked to their discs. Herbst et al. (2002) argue that this is because stars are released from disc locking after around 1 Myr. However, the period distribution is also consistent with stars *becoming* locked to their discs after around 1 Myr. In the discussion to follow, we will refer to these as scenarios one and two, respectively. There may be some justification for preferring scenario two, as Hartmann (2002) suggests that disc locking can only spin-down stars as rapidly as angular momentum can be removed from the inner disc, implying that young stars may indeed not be locked to their discs for the early stages of their lives. However, the claims of Hartmann (2002) are challenged by (?), who perform a more detailed analysis and find that the time taken to lock a young star to its disc should be at most  $4 \times 10^5$  yr, much shorter than that claimed by Hartmann (2002), and less than the  $\sim 1$  Myr age of the ONC. It is therefore an open question whether theoretical predictions prefer scenario one or two.

A challenge to the explanation of rotation rates of stars in Orion through a disc locking paradigm is apparently posed by the period distribution in the Orion flanking fields. Although the flanking fields also show signs of bi-modality (the Hartigan dip test gives only a 10% chance of unimodality), the distribution of periods themselves are noticeably different. This is surprising, because there is no evidence that the flanking fields differ in age from the ONC. The largest difference is that the peak of slow rotators has shifted from 8 days to 6 days. This difference in distributions is statistically significant (a K-S test gives a 0.5% chance of the two being drawn from the same parent distribution). However, this apparent problem has a natural explanation under the disc locking paradigm. The disc fraction as measured by K-band excess in the OFF is significantly lower at 15% (Rebull 2001) than that reported for the ONC at 50% (Hillenbrand 1997). Given the lower disc fractions, it is reasonable to assume that the discs in the OFF are less massive, and therefore less efficient at braking the young stars than those in the ONC. Under scenario one, the slow rotators in Orion would have become unlocked earlier from these low mass discs, and have hence spun up from eight to six days. Assuming that the radius of the star changes as  $R \propto t^{-1/3}$ , a star locked to its disc at a period of 8 days would have to have been released from disc locking at around 0.6 Myr, in order to have

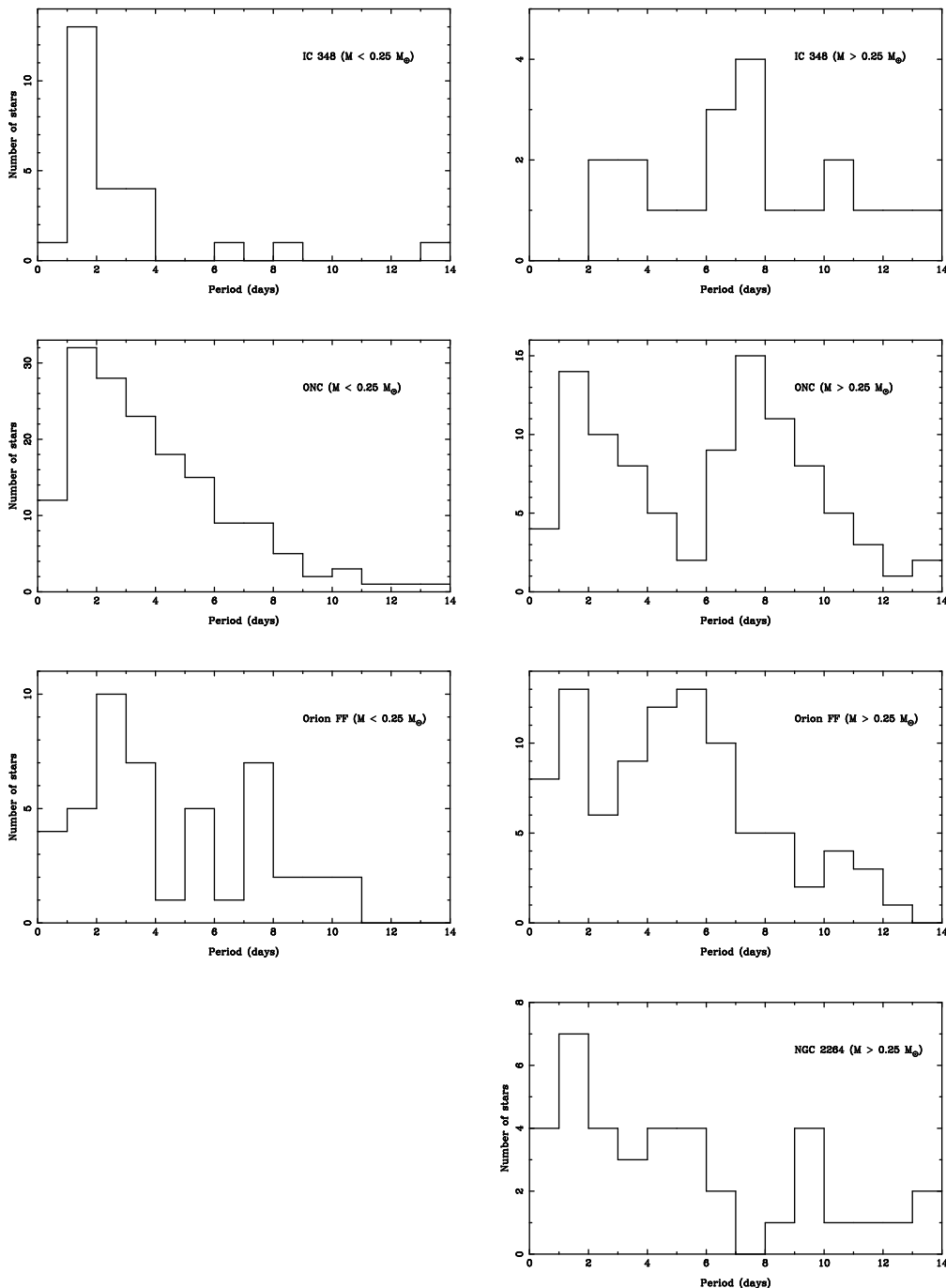


**Figure 10.** Distribution of periods in IC 348 compared with the distributions for the ONC (Herbst et al. 2002), Orion flanking fields (Rebull 2001) and NGC 2264 (Makidon et al. 2004). Masses in the ONC have been assigned by Hillenbrand (1997) using the isochrones of D’Antona & Mazzitelli (1994). Masses in IC 348 have been assigned using the effective temperatures and luminosities of Luhman et al. (2003), and the isochrones of D’Antona & Mazzitelli (1997). Identical period distributions are produced for IC 348 if the D’Antona & Mazzitelli (1994) isochrones are used. Masses for the stars in NGC 2264 were assigned by Makidon et al. (2004), following the method of Hillenbrand (1997). We assigned masses to the stars in the Orion Flanking fields using the spectral types and extinctions from Rebull (2001), and following the method of Hillenbrand (1997).

a period of 6 days at 1 Myr. Under scenario two, the stars in the OFF will have become locked relatively late to their less massive discs, and have not yet had time to become fully locked. Using the data from Orion alone, it is not possible to distinguish between the two scenarios.

One possible way to resolve this degeneracy is to look

at the rotation rates for older clusters. If discs are initially locked, and then released after  $\sim 1$  Myr, then we would expect stars to spin-up, and the period distribution should be more strongly biased towards fast rotators than seen in the ONC. Alternatively, if disc locking only becomes effective after about 1 Myr, then the period distribution of older clus-

ters should show fewer fast rotators than seen even in the ONC. Unfortunately, the period distributions of older clusters are contradictory. IC 348 shows a large number of slow rotators (around 8 days), and very few fast rotators (there are no period found below 2 days). This dearth of fast rotators was first commented on by Herbst et al. (2000), but their result was not significant, due to small number statistics, and a possible lack of sensitivity to the shortest periods. To assess the significance of the lack of fast rotators in this study, we selected twenty high-mass stars at random from the ONC dataset. This produced a sub-sample of the ONC data which was the same size as our high-mass sample in IC 348. In 98% of tests this sub-sample had one or more stars with periods below two days. We therefore conclude that the lack of fast rotators in IC 348 is significant. Taken in isolation, this result would suggest that the ONC, OFF and IC 348 data could be explained in a cohesive picture of disc-locking, in which disc locking took  $\sim 1$  Myr to become effective. At the age of IC 348 (approx 3 Myr) disc locking has further removed fast rotators, and increased the percentage of stars rotating near 8 days. However, there are two problems with this picture. The first problem is posed by the lack of any correlation between IR excess and rotation rate in IC 348, and the uncertainty as to the true cause of the correlation found in the ONC. A lack of a correlation between signatures of disc presence and rotation rate is a major challenge to disc-locking theory. The second problem is posed by the period distribution of NGC 2264. At a similar age and disc fraction to IC 348, we might expect NGC 2264 to show similar rotation properties. Instead, the period distribution in NGC 2264 is more strongly skewed towards fast rotators than the ONC! K-S tests reveal that whilst the NGC 2264 distribution is not statistically different from the OFF, it is different from the ONC and IC 348 (at 96% and 99.6% confidence levels respectively). This result is in direct opposition with the result for IC 348, and causes serious difficulties for disc locking. Given that NGC 2264 and IC 348 show very similar ages distributions and disc fractions, disc locking theory provides no explanation for the marked difference in period distributions. We must therefore also conclude that if disc locking does regulate angular momentum in young stars, differences between cluster environments mask many of the observational effects of that regulation.

## 5.2 Stars with masses less than $0.25 M_{\odot}$

In both IC 348 and the ONC, the period distribution of the low-mass stars is markedly different to that of the high mass stars. Why this should be the case is uncertain. Interpreted in the context of disc locking, either the low-mass stars are not locked to their discs, are locked to their discs for a short amount of time, or are locked to their discs at shorter locking periods than the high mass stars. Examination of the period distributions for IC 348 and the ONC seems to rule out this latter possibility. If we assume that IC 348 evolved from an ONC-like period distribution then it is clear that the high mass stars have spun down, whilst the low-mass stars have spun up. This is not consistent with the low-mass stars having their angular momenta regulated in the same way as the high-mass stars. Short disc lifetimes, or a mechanism to reduce the effectiveness of disc locking, are therefore

necessary to explain the period distributions of the low mass stars. This implies either a difference in magnetic field properties, or in disc properties between the high and low mass stars. Currently, little is known about the magnetic fields in young stars, or how they behave with stellar mass. However, disc truncation by stellar encounters suggests a difference in disc properties between low and high mass stars. If low-mass stars are the results of frequent stellar encounters, they will possess relatively low mass discs (Bate et al. 2003). These discs will be inefficient at regulating stellar angular momentum. We might therefore expect the low-mass stars angular momentum evolution to be characterised by steady spin-up. This is the case in IC 348 - although the high mass stars show a dearth of fast rotators compared to the ONC, the low mass stars in IC 348 are rotating very rapidly indeed, with the vast majority of stars having periods around 1–2 days. The obvious conclusion is that the discs around low-mass stars do not regulate the stellar angular momentum in the same way as discs around high mass stars do. An excellent test of this suggestion will be the low-mass period distribution for NGC 2264. Even though the high mass period distribution is very different to IC 348 the above hypothesis suggests that the low-mass distribution will be quite similar.

## 5.3 Disc locking and infrared excess

A major challenge to any interpretation of period distributions in terms of disc locking is presented by the lack of any reliable correlation between disc indicators such as infrared excess and rotation rate in any of the clusters presented here. In the absence of any such correlation it is tempting to say that disc locking cannot be responsible for regulating the angular momentum of young stars. This is not necessarily the case, however, and two alternative possibilities are outlined below.

- The intrinsic spread in indicators might mask any correlation between rotation rate and rotational period. Inclination effects and the effects of inner disc holes can produce a large spread in the size of any infrared excess (Hillenbrand et al. 1998).
- The disc indicators could be *too sensitive*. If high mass discs are needed to effectively regulate a star's rotation, then the presence of an K-band or L-band excess does not necessarily imply a disc of sufficient mass. Discs with masses as small as  $10^{-5} M_{\odot}$  can produce a detectable K-band excess (Wood et al. 2002).

## 6 CONCLUSIONS

We have presented a photometric study of rotation rates in the young cluster IC 348. The depth and temporal density of our observations has allowed us to (i) more than double the known number of periodic stars associated with the cluster, (ii) discover periods in stars with masses less than  $0.25 M_{\odot}$  and (iii) discover periods in classical T-Tauri stars for the first time in this cluster. The period distribution of stars with masses greater than  $0.25 M_{\odot}$  shows the same bi-modal behaviour as seen in the ONC, although there is a statistically significant lack of rapidly rotating stars with respect to Orion.

We have also presented a discussion of our data in the context of previously published period distributions for the ONC, Orion flanking fields and NGC 2264. We find two significant problems with the disc locking paradigm.

- We find that the previously claimed correlation between infrared excess and rotation period in the ONC might in fact result from a correlation between infrared excess and *mass*.
- We also find a marked difference in period distributions between NGC 2264 and IC 348, which presents a serious challenge to the disc locking paradigm, given the similarity in ages and disc fractions between the two clusters.

#### ACKNOWLEDGEMENTS

SPL is supported by PPARC. The authors acknowledge the data analysis facilities at Exeter provided by the Starlink Project which is run by CCLRC on behalf of PPARC. We thank W. Herbst for providing the data in Cohen et al. (2004) prior to publication, and J. Pringle for useful discussions.

#### REFERENCES

- Attridge J. M., Herbst W., 1992, ApJ, 398, L61  
 Barnes S., Sofia S., Pinsonneault M., 2001, ApJ, 548, 1071  
 Bate M. R., Bonnell I. A., Bromm V., 2003, MNRAS, 339, 577  
 Bouvier J., Appenzeller I., 1992, A&AS, 92, 516  
 Bouvier J., Cabrit S., Fernandez M., Martin E. L., Matthews J. M., 1993, A&A, 272, 176  
 Burningham B., Naylor T., Jeffries R. D., Devey C. R., 2003, MNRAS, 346, 1143  
 Choi P. I., Herbst W., 1996, AJ, 111, 283  
 Cohen R. E., Herbst W., Williams E. C., 2004, AJ, 127, 1602  
 D'Antona F., Mazzitelli I., 1994, ApJS, 90, 467  
 D'Antona F., Mazzitelli I., 1997, Mem. Soc. Astr. It., 68, 807  
 Edwards S., Strom S. E., Hartigan P., Strom K. M., Hillenbrand L. A., Herbst W., Attridge J., Merrill K. M., Probst R., Gatley I., 1993, AJ, 106, 372  
 Gregorio-Hetem J., Hetem A., 2002, MNRAS, 336, 197  
 Haisch K. E., Lada E. A., Lada C. J., 2001, AJ, 121, 2065  
 Hamilton C. M., Herbst W., Shih C., Ferro A. J., 2001, ApJ, 554, L201  
 Hartigan J. A., Hartigan P., 1995, Ann. Statist., 13, 70  
 Hartigan P., 1995, Appl. Statist., 13, 70  
 Hartmann L., 2002, ApJ, 566, L29  
 Herbig G. H., 1998, ApJ, 497, 736  
 Herbst W., Hamilton C. M., Vrba F. J., Ibrahimov M. A., Bailer-Jones C. A. L., Mundt R., Lamm M., Mazeh T., Webster Z. T., Haisch K. E., Williams E. C., Rhodes A. H., Balonek T. J., Scholz A., Riffeser A., 2002, PASP, 114, 1167  
 Herbst W., Herbst D. K., Grossman E. J., Weinstein D., 1994, AJ, 108, 1906  
 Herbst W., Maley J. A., Williams E. C., 2000, AJ, 120, 349  
 Herbst W., Wittenmyer R., 1996, Bulletin of the American Astronomical Society, 28, 1338  
 Hillenbrand L. A., 1997, AJ, 113, 1733  
 Hillenbrand L. A., Strom S. E., Calvet N., Merrill K. M., Gatley I., Makidon R. B., Meyer M. R., Skrutskie M. F., 1998, AJ, 116, 1816  
 Horne J. H., Baliunas S. L., 1986, ApJ, 302, 757  
 Johns-Krull C. M., Valenti J. A., Koresko C., 1999, ApJ, 516, 900  
 Koenigl A., 1991, ApJ, 370, L39  
 Lamm M. H., Bailer-Jones C. A. L., Mundt R., Herbst W., Scholz A., 2004, A&A, 417, 557  
 Landolt A. U., 1992, AJ, 104, 340  
 Linnell Nemec A. F., Nemec J. M., 1985, AJ, 90, 2317  
 Littlefair S. P., Naylor T., Harries T. J., Retter A., O'Toole S., 2004, MNRAS, 347, 937  
 Luhman K. L., Stauffer J. R., Muench A. A., Rieke G. H., Lada E. A., Bouvier J., Lada C. J., 2003, ApJ, 593, 1093  
 Makidon R. B., Rebull L. M., Strom S. E., Adams M. T., Patten B. M., 2004, AJ, 127, 2228  
 Matt S., Pudritz R. E., 2004, ApJ, 607, L43  
 Naylor T., 1998, MNRAS, 296, 339  
 Naylor T., Totten E. J., Jeffries R. D., Pozzo M., Devey C. R., Thompson S. A., 2002, MNRAS, 335, 291  
 Rebull L. M., 2001, AJ, 121, 1676  
 Rebull L. M., Makidon R. B., Strom S. E., Hillenbrand L. A., Birmingham A., Patten B. M., Jones B. F., Yagi H., Adams M. T., 2002, AJ, 123, 1528  
 Safer P. N., 1998, ApJ, 494, 336  
 Scholz R.-D., Brunzendorf J., Ivanov G., Kharchenko N., Lasker B., Meusinger H., Preibisch T., Schilbach E., Zinnecker H., 1999, A&AS, 137, 305  
 Stassun K. G., Mathieu R. D., Mazeh T., Vrba F. J., 1999, AJ, 117, 2941  
 Tinker J., Pinsonneault M., Terndrup D., 2002, ApJ, 564, 877  
 Wood K., Lada C. J., Bjorkman J. E., Kenyon S. J., Whitney B., Wolff M. J., 2002, ApJ, 567, 1183